Highly Flexible Electronic and Optical Films Composed of Hydrophobic and Hydrophilic Multilayers[a]

Sungwoo Kim, Bokyoung Lee, Sanghyo Kim, Joona Bang, Jinhan Cho*

We introduce a novel and efficient strategy for producing free-standing functional films via photo-crosslinking and electrostatic layer-by-layer (LbL) assembly, which can allow the build-up of hydrophilic multilayers onto hydrophobic surfaces. Hydrophobic multilayers were deposited on ionic substrates by a photo-crosslinking LbL process using photo-crosslinkable polymers. The photo-crosslinked surface was converted to an anionic surface by excess UV light irradiation. This treatment allowed also the stable adhesion between metal electrode or cationic polyelectrolyte and hydrophobic multilayers. After dissolving the ionic substrates in water, the formed free-standing films exhibited unique functionalities of inserted components within hydrophobic and/or hydrophilic multilayers.

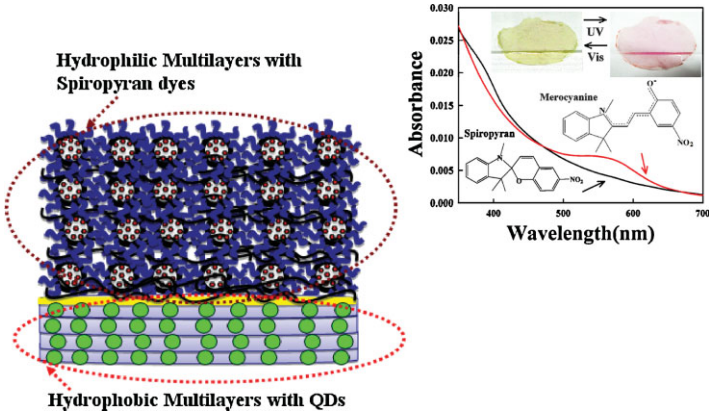

Introduction

Free-standing functional films using solution processes have attracted considerable attention for their many novel applications, such as membranes,[1] mechanically reinforced nanocomposite films,[2] or wearable electronic systems[3] with simple and facile routes. Although various approaches for the free-standing films, such as the sol–gel process,[4] self-assembly of block copolymers,[5] or layer-by-layer (LbL) assembly method,[1,2,6–9] have been introduced, it is essential to develop novel strategies that allow a high degree of control over the film/layer dimensions (from the angstrom to the μm level), flexibility control and the facile detachment of films while at the same time allowing the incorporation of a different chemistry of the hydrophobic/hydrophilic balance.

Among several methods, the LbL assembly method offers a wide range of opportunities for preparing nanocomposite films with a controlled thickness, composition, and functionality through complementary interactions (i.e., electrostatic, hydrogen-bonding, or covalent interaction).[10–14] However, the conventional LbL method itself has inherent limitations on increasing the individual layer thickness significantly in a single deposition step. For example, in the case of fabricating LbL multilayer films with a micron-scale thickness for functional free-standing films,[2,11] these films should have hundreds of layers

J. Cho, S. Kim, B. Lee, S. Kim
School of Advanced Materials Engineering, Kookmin University, Jeongneung-dong, Seongbuk-gu, Seoul 136-702, Korea
E-mail: jinhan@kookmin.ac.kr
S. Kim
College of BioNano Technology, Kyungwon University, San 65, Bokjeong-dong, Sujeong-gu, Kwonggi-do 461-701, Korea
J. Bang
Department of Chemical and Biological Engineering, Korea University, Anam-dong, Sungbuk-gu, Seoul 136-713, Korea

[a] Supporting information for this article is available at the bottom of the article's abstract page, which can be accessed from the journal's homepage at http://www.mcp-journal.de, or from the author.

Macromol. Chem. Phys. **2010**, *211*, 1188–1195

DOI: 10.1002/macp.201000104

because the layer adsorbed from a single deposition process has only a few nanometer thickness after rinsing. Recently, it was reported that hydrophobic polymers and/or nanoparticles containing photo-crosslinking units can be deposited consecutively onto ionic substrates, allowing a range of length-scales from a few angstrom (Å) to a hundred nanometers (nm) thickness per layer. Moreover, these hybrid nanocomposite multilayers could be separated by dissolving the substrates in aqueous media.[15,16] Although this approach has an important advantage in preparing free-standing films with micron-scale thickness and hydrophobic properties without physical/chemical damage, there is considerable difficulty in assembling hydrophilic components electrostatically onto hydrophobic multilayer-coated ionic substrates. Therefore, in order for our approach to be generalized as an effective process for free-standing functional films, the photo-crosslinking LbL process for hydrophobic free-standing multilayers should be completely compatible with the conventional LbL process for hydrophilic multilayers onto a defined or patterned area.

Herein, we introduce a novel process for depositing free-standing nanocomposite films composed of hydrophobic and hydrophilic multilayers. The strategy is based on the conversion of a photo-crosslinked surface to a hydrophilic surface by excess exposure to UV light irradiation. This surface treatment allows electrostatically charged materials to be assembled onto photo-crosslinked multilayers without any dissolution of the NaCl substrates. In addition, when electrochemical sensing components are incorporated into electrostatic multilayers, the resulting free-standing films obtained after removing the NaCl substrates exhibit electrochemical activities toward the probing materials. Furthermore, it is shown that multi-functional optical films can be prepared through combination of the hydrophobic multilayers containing fluorescent quantum dot (QD) and the hydrophilic multilayers with photochromic dyes. These results also demonstrate the possibility of selective LbL growth onto patterned regions based on electrostatic interactions using a UV-photomask. Considering that a variety of hydrophobic and hydrophilic components can be incorporated easily into electrostatic LbL-assembled films with controllable flexibility and tailored functionalities, it is believed that this approach can provide a facile route to potential applications, such as highly flexible displays or electronics.

Experimental Part

Materials

Photo-crosslinkable polystyrene, PS-N_3 ($\overline{M}_n = 28.0\,kg \cdot mol^{-1}$) with approximately 10 wt.-% UV-sensitive azide groups ($-N_3$) was synthesized via reversible addition fragmentation transfer (RAFT) polymerization as reported in ref.[10,11] The thiol terminated random copolymers, PS$-N_3-$SH ($\overline{M}_n = 6.5\,kg \cdot mol^{-1}$), was synthesized by the similar procedure as PS$-N_3$. The only difference is the reaction with AIBN was replaced by the reaction with hexylamine to convert the dithioester group to the thiol group (see Supporting Information, Figure S1).

For the preparation of photo-crosslinkable QDs(PS$-N_3-$SH$-$QDs), oleic acid-stabilized CdSe@ZnS with green emissive color was first synthesized. For green emissive QDs of about 5.0 nm size, 30 mg of CdO, 733 mg of zinc acetate, 4 mL of oleic acid, and 15 mL of 1-octadecene were put into a 310 mL round flask. The mixture was heated to 150 °C with N_2 gas blowing, and further heated to 310 °C to form a clear solution of $Cd(OA)_2$ and $Zn(OA)_2$. At this temperature, 15.8 mg of Se powder and 128.4 mg of S powder both dissolved in 3 mL of trioctylphosphine were quickly injected into the reaction flask. After the injection, the temperature of the reaction flask was set to 300 °C for promoting the growth of QDs, and it was then cooled to room temperature to stop the growth. QDs were purified by adding 20 mL of chloroform and an excess amount of acetone (three times). After this purification, PS$-N_3-$SH of 2 wt.-% was added to QD solution of 15 mL for the stabilizer exchange from oleic acid to PS$-N_3-$SH and then was heated at 40 °C for 2 h. QDs were purified by adding 20 mL of chloroform and an excess amount of acetone (three times). After this purification, PS$-N_3-$SH of 2 wt.-% was added to QD solution of 15 mL for the stabilizer exchange from oleic acid to PS$-N_3-$SH and then was heated at 40 °C for 2 h.

For the preparation of negatively charged PS_{61K}-*b*-PAA_{4K} micelles in water, 100 mg of PS_{61K}-*b*-PAA_{4K} block copolymer and 2 mg of water-insoluble photochromic dyes (spiropyran) were first dissolved in 4 mL of *N,N*-dimethylformamide (DMF), which was followed by the addition of 96 mL of water (pH 10.0), resulting in spherical block copolymer micelles (BCMs) composed of a hydrophobic PS core and a negatively charged PAA corona shell.

PS$-N_3$ and PS$-N_3$–SH$-$QD:PS$-N_3$ Multilayers

For the build-up of multilayer films, the PS$-N_3$ solution of 4 wt.-% or mixed solution of PS$-N_3-$SH$-$QD (1 wt.-% for QD and 2 wt.-% for PS$-N_3-$SH) and PS$-N_3$ (2 wt.-%) was wetted completely on quartz, silicon, or NaCl substrates. The substrate was then rotated at 3 000 rpm for 20 s with a spinner, and the resulting films were photo-crosslinked by UV irradiation ($\lambda = 254$ nm) for 60 s. The subsequent layers were also deposited sequentially onto the previous films using the same procedure. In the case of free-standing films, multilayers were deposited sequentially onto NaCl substrates with repetitive thermal cross-linking.

(PAH/spiropyran-BCM)$_n$ and (PAH/CAT)$_n$ onto PS$-N_3$ or PS$-N_3-$SH$-$QD:PS$-N_3$ Multilayer-Coated NaCl

The $(PS-N_3)_{30}$ or $(PS-N_3-SH-QD{:}PS-N_3)_{30}$ multilayer-coated NaCl substrates were irradiated with UV radiation ($\lambda = 254$ nm) for 120 s. After this photo-treatment, the surface of the PS$-N_3$ multilayers was converted into a negatively charged surface. For the build-up of $(PAH/CAT)_n$ multilayers, a positively charged PAH solution (1 mg $\cdot$ mL^{-1}, pH 9) was wetted onto Pt-coated $(PS-N_3)_{30}$ multilayers. The substrate was then rotated with a spinner at

3 000 rpm for 20 s and then spin-rinsed with deionized water at the same spinning speed and time. A negatively charged CAT solution was also deposited sequentially onto the substrates using the same procedure mentioned above. These processes were repeated up to the formation of 30 bilayers, and were identical to those used for the preparation of $(PAH/spiropyran\text{-}BCM)_n$ multilayers onto $(PS{-}N_3{-}SH{-}QD{:}PS{-}N_3)_{30}$ multilayer-coated substrates.

Measurements

The Fourier UV–Vis spectra were obtained using a Perkin Elmer Lambda 35 UV–Vis spectrometer. A QCM device (QCM200, SRS) was used to examine the mass of material deposited after each adsorption step. The resonance frequency of the QCM electrodes was approximately 5 MHz. The adsorbed mass of PAH and spiropyran-BCM, Δm, can be calculated from the change in QCM frequency, ΔF, using the Sauerbrey equation: $\Delta F\ (\mathrm{Hz}) = -56.6 \times \Delta m_A$, where Δm_A is the mass change per quartz crystal unit area, in $\mu g \cdot cm^{-2}$.[17] The size of BCM with and without spiropyran was measured by TEM (model: JEM-2000EXII). The FTIR spectra were obtained using a FTIR-200 spectrometer (JASCO corporation).

Results and Discussion

Electrochemical Films

Free-standing electrochemical films were deposited on $(PS\text{-}N_3)_{30}$-coated NaCl substrates. Figure 1a shows a schematic diagram of the process for preparing free-standing electrochemical sensing films composed of hydrophobic $(PS{-}N_3)_n$ and $(PAH/CAT)_n$ multilayers. The experimental details for the preparation of photo-crosslinkable $PS{-}N_3$ was given in Experimental Section and Supplementary Information (Figure S1). First, for the preparation of hydrophobic multilayers, a 4 wt.-% $PS{-}N_3$ solution containing 10 wt.-% azide groups was spin-deposited onto ionic substrates at a spin speed of 3 000 rpm and consecutively photo-crosslinked under UV light irradiation at 254 nm for 60 s. The measured thickness of the $PS{-}N_3$ per layer was approximately 200 nm. In addition, it was reported that the mechanical properties of $PS{-}N_3$ measured from depth-sensing indentation experiments was similar to those of a pure PS layer (approximately 4.35 GPa for the elastic modulus and 0.51 GPa for hardness).[15] After consecutively depositing the photo-crosslinked layers up to 30 layers, the films were exposed to excess UV light for 120 s to generate a range of oxygen-containing functional units, such as C–O, C=O, and COOH (or COO^-) from hydrophobic styrene groups.[18,19] In this case, the contact angles of the water droplets on $PS{-}N_3$ multilayers decreased significantly from 92° to approximately 60° with increasing UV irradiation time from 0 to 120 s, as shown in Figure 1b. After this UV treatment, the Pt layer as a bottom electrode was deposited preferentially onto PS-N_3 multilayers using a conventional sputtering process. Stable adhesion between the Pt electrodes and photo-crosslinked multilayers was formed due to the presence of nitrogen atoms within the multilayers[16] and furthermore the additional UV treatment was performed for the hydrophilic surface of Pt electrode. This suggests that electrostatic charged multilayers showing electrochemical sensing properties can be subsequently deposited onto Pt-coated PS-N_3 multilayers.

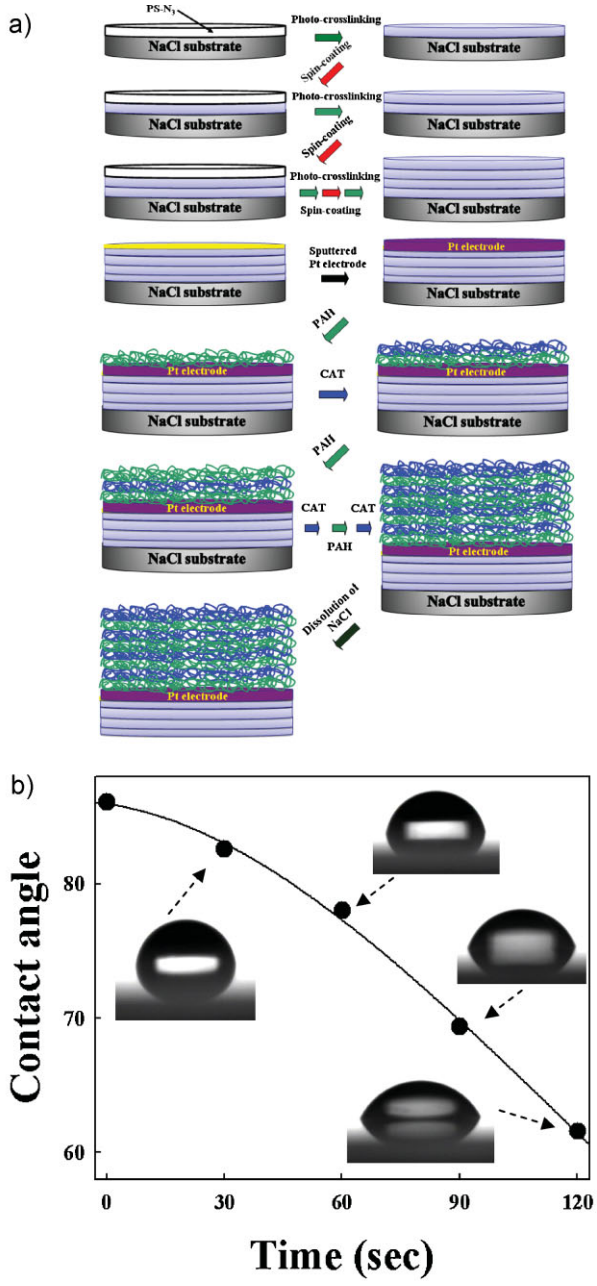

Figure 1. (a) Schematics to prepare free-standing electrochemical sensing films composed of hydrophobic $PS{-}N_3$ and hydrophilic PAH/CAT multilayers. (b) Water contact angles measured from $PS{-}N_3$ multilayers with increasing the irradiation time of excess UV light from 0 to 120 s.

Macromol. Chem. Phys. **2010**, *211*, 1188–1195

Macromolecular Journals

DOI: 10.1002/macp.201000104

Generally, CAT is an efficient catalysts for H_2O_2 and bears an overall positive charge at pH < 5.6 and negative charge at pH > 5.6 (i.e. isoelectric point, $pI \approx 5.6$). Therefore, it was envisioned that electrostatic multilayer films composed of PAH and CAT could exhibit electrochemical behavior toward H_2O_2.[20–25] The amount of PAH and CAT adsorbed onto anionic QCM electrodes during LbL self-assembly at pH 9/9 was first investigated. Under this pH, the amounts of PAH and CAT adsorbed per bilayer were approximately 360 $ng \cdot cm^{-2}$ (frequency change, $\Delta F \approx 20.4 \pm 2$ Hz) and 397 $ng \cdot cm^{-2}$ ($\Delta F \approx 22.5 \pm 2$ Hz), respectively (Figure 2a). Moreover, the uniform growth of adsorbed mass (or frequency change) indicates that the amount of CAT adsorbed per bilayer is regular. Based on these results, $(PAH/CAT)_{10}$ multilayers were deposited onto a Pt-coated substrate, and the subsequent dissolution of the NaCl substrate produced highly flexible films allowing electrochemical sensing toward hydrogen peroxide (H_2O_2), as shown in Figure 2b. The curves in Figure 2c show the cyclic voltammograms (CVs) of free-standing PAH/CAT multilayer-coated films for sensing H_2O_2 gas at scan rate of 50 $mV \cdot s^{-1}$. The relatively weak redox reaction shown in 0 mM H_2O_2 is due to the redox process of the Fe^{2+}/Fe^{3+} couple in the iron heme structure of CAT. On the other hand, the electrode modified with the PAH/CAT multilayers showed a notable increase in the reduction peak at approximately −0.3–0.37 V, as well as a slight increase in the oxidation peak potential at 0.2 V with increasing H_2O_2 concentration from 5 to 15 mM. This suggests that CAT has catalytic activity toward H_2O_2. In addition, the redox peak currents showed a linear dependence on the H_2O_2 concentration (Figure 2c). These phenomena were more evidently shown in two calibration curves corresponding to amperometric responses (Figure 2d). Although the overall mechanism of the electrocatalytic process was not revealed clearly, the proposed mechanism is as follows. When H_2O_2 enters the iron heme group in CAT (i.e., Fe^{III}-CAT), a reactive oxidant with a cation radical on the heme porphyrin (i.e., $O=Fe^{IV}$-CAT $\cdot^+$) is formed that sequen-

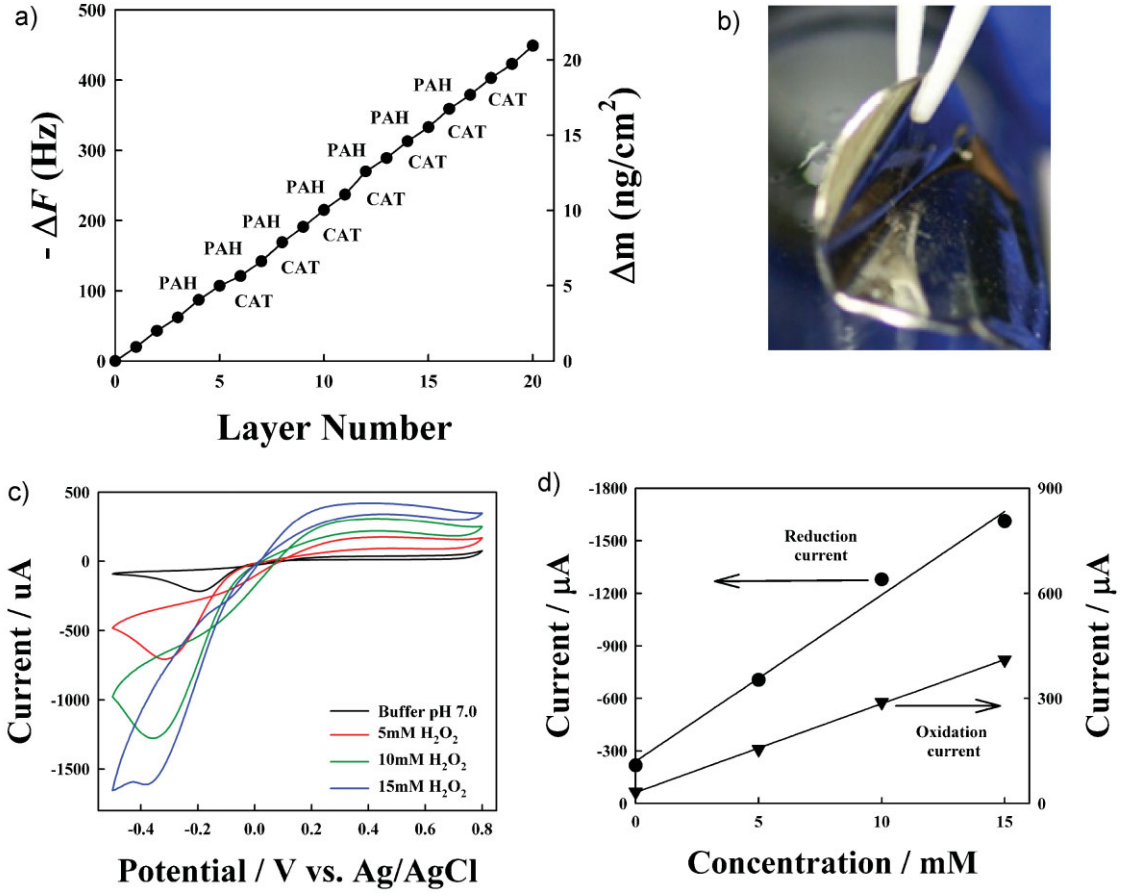

Figure 2. (a) Frequency changes as a function of layers for the assembly of PAH/CAT films on a PS−N_3-coated QCM electrode. (b) Digital camera image of free-standing electrochemical sensing films (i.e., $(PAH/CAT)_{10}/Pt/(PS-N_3)_{30}$ multilayers) obtained after dissolving ionic substrates in aqueous medium. (c) CVs of free-standing $(PAH/CAT)_{10}$-modified Pt electrode in pH 7.0 PBS containing 0, 5, 10, and 15 mM H_2O_2 at a scan rate of 50 $mV \cdot s^{-1}$. (d) Calibration curves of the amperometric responses of flexible Pt electrodes modified with $(PAH/CAT)_{10}$ multilayers.

tially accepts an electron from H_2O_2 to form a nonradical compound (i.e., $O{=}Fe^{IV}$-CAT), resulting in the oxidation of H_2O_2. A nonradical compound can further accept a second electron to regenerate Fe^{III}-CAT, which causes the reduction peak current.[25]

Free-standing film devices can be prepared easily without adverse effects on the inherent properties (i.e., optical or electrochemical sensing properties) of the functional multilayers, and a variety of components ranging from hydrophilic to hydrophobic materials can be integrated effectively into the nanostructured films. Furthermore, this approach can allow the uniform growth of electrostatic multilayer films on the selective domains of PS-N_3 multilayer-coated substrates, which suggests almost complete conformity with the typical LbL techniques developed thus far (see Supporting Information, Figure S2).

Optical Films

As shown in free-standing electrochemical films, photo-crosslinking-induced hydrophobic multilayers were used as only substrates. However, our approach is very effective for preparing nanocomposite multilayers with multifunctional properties, in that a variety of components ranging from hydrophobic to hydrophilic materials can be easily inserted within multilayers. For demonstrating this possibility, the nanocomposite multilayer films with dual optical properties were fabricated using photo-crosslinking and electrostatic LbL assembly. Figure 3 shows a schematic diagram of the process for preparing free-standing optical films composed of photoluminescent QDs-incorporated hydrophobic multilayers (i.e., $(PS{-}N_3{-}SH{-}QDs{:}PS{-}N_3)_n$) and photochromic dye-incorporated hydrophilic multilayers (i.e., $(PAH/spiropyran\text{-}BCM)_n$). The experimental details for the preparation of photo-crosslinkable $PS{-}N_3{-}SH{-}QDs{:}PS{-}N_3$ and negatively charged siropyran-BCMs were given in the Experimental Sections and Supporting Information (Figure S3).

The deposition process for the build-up of $(PS{-}N_3{-}SH{-}QDs{:}PS{-}N_3)_{30}$ multilayers and the excess UV treatment were identical to that used for $(PS{-}N_3{-}SH{-}QD{:}PS{-}N_3)_{30}$ multilayer-coated substrates. In this case, positively charged PAH, which was adjusted to a solution pH of 9, was spin-assembled onto $PS{-}N_3$ multilayers at a spinning speed of 3 000 rpm and consecutively spin-rinsed with deionized water at the same spinning speed. After depositing the cationic PAH, the negatively charged spiropyran-BCMs at pH 9 were deposited using the abovementioned procedure [*In this case, the diameter of BCM was increased from approximately 86 nm (BCM without spiropyran dyes) to 118 nm after incorporating the water-insoluble spiropyran dyes into the hydrophobic PS core block* (Figure 4a)]. The consecutive spin-deposition and electrostatic interaction between $-NH_3^+$ ($pK_a \approx 10$) of PAH and the

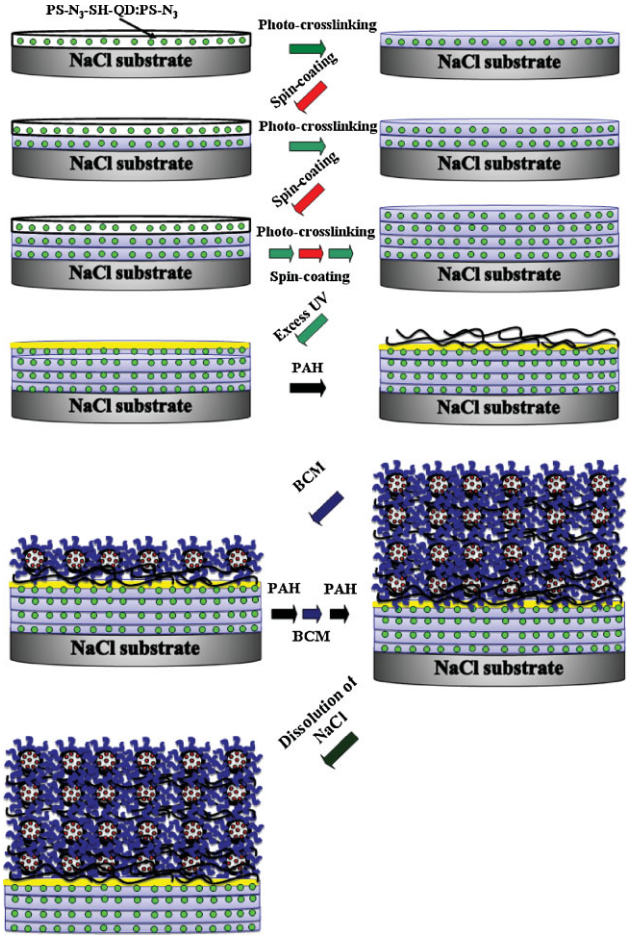

Figure 3. Schematics to prepare free-standing optical films composed of hydrophobic $(PS{-}N_3{-}SH{-}QD{:}PS{-}N_3)_n$ and hydrophilic $(PAH/spiropyran\text{-}BCM)_n$ multilayers.

$-COO^-$ groups of the PAA corona chains ($pK_a \approx 4.5$) in spiropyran-BCMs at pH 9 can induce the build-up of hydrophilic multilayers (see Supporting Information, Figure S4).[26–29] Quartz crystal microgravimetry (QCM) measurements were carried out to determine the amount of PAH and spiropyran-BCMs adsorbed in the multilayer films. Based on the mass changes calculated from the frequency changes,[17] the alternate deposition of PAH and spiropyran-BCMs resulted in a $-\Delta m$ of ≈ 263 ng $\cdot$ cm^{-2} ($-\Delta F$ of 15 ± 2) and ≈ 378 ng $\cdot$ cm^{-2} ($-\Delta F$ of 21 ± 2 Hz), respectively (Figure 4b). UV–Vis spectroscopy also confirmed that the amounts adsorbed onto the $PS{-}N_3{-}SH{-}QD{:}PS{-}N_3$–coated substrates were similar to those onto the bare substrates except for a slight difference in the amount adsorbed in the first layers (see Supporting Information, Figure S5).

Based on these results, we examined the photoluminescent (PL) behavior of $PS{-}N_3{-}SH{-}QD{:}PS{-}N_3$ multilayers and the photochromic properties of PAH/spiropyran-BCM multilayers including water-insoluble spiropyrans, which

Macromol. Chem. Phys. **2010**, *211*, 1188–1195

Macromolecular Journals

DOI: 10.1002/macp.201000104

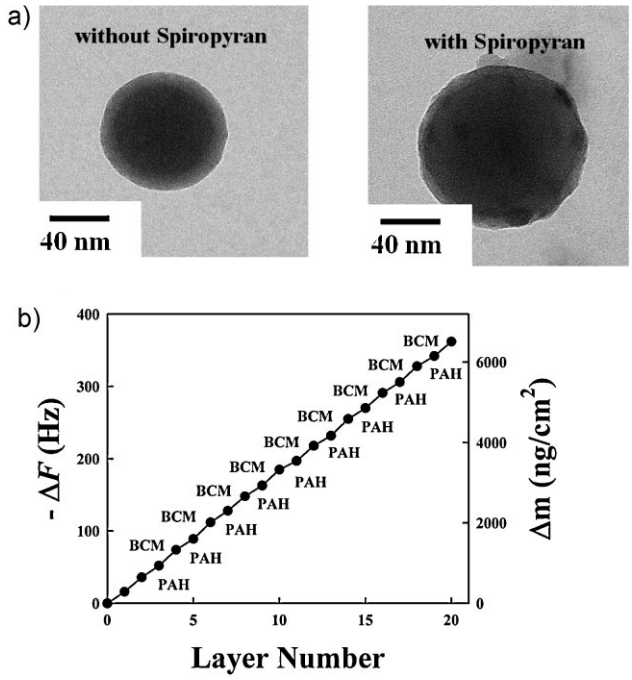

Figure 4. (a) TEM images of BCMs without and with spiropyran dyes. These water-insoluble dyes were incorporated into hydrophobic PS core block of BCMs. (b) Frequency changes as a function of layers for the assembly of PAH/spiropyran-BCM films on a PS–N_3-coated QCM electrode. The mass changes calculated from the frequency changes: ΔF (Hz) $= -56.6 \times \Delta m_A$, where Δm_A is the mass change per quartz crystal unit area, in $\mu g \cdot cm^{-2}$.

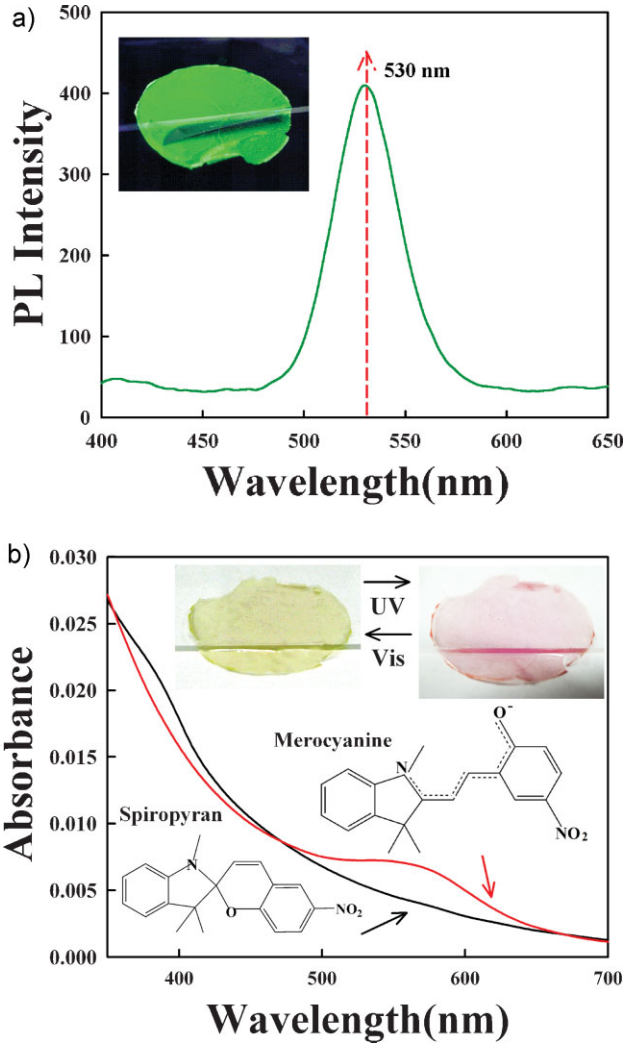

Figure 5. (a) PL and (b) UV–Vis spectra free-standing optical films composed of hydrophobic (PS–N_3–SH–QD:PS–N_3)$_n$ and hydrophilic (PAH/spiropyran-BCM)$_n$ multilayers. The insets of (a) and (b) display the photographic images taken from digital camera. The PL spectrum was measured at excitation wavelength of 350 nm and the change in UV–Vis spectra occurred from (PAH/spiropyran-BCM)$_{10}$ multilayer films UV irradiation at 365 nm.

have the QD-induced luminescence by UV irradiation and the light-induced reversible isomerization between the colorless spiropyran (after visible light) and colored forms of merocyanines (after UV light irradiation), respectively.[29,30] Our approach using QDs and BCMs allows the production of PL and photochromic intensity-tunable films loaded with CdSe@ZnS and spiropyran. Figure 5a shows the photographic image and PL spectrum of about 3 μm thick free-standing multilayers composed of (PS–N_3–SH–QD:PS–N_3)$_{30}$ and (PAH/spiropyran-BCM)$_{10}$ multilayers at excitation wavelength of 350 nm. In this case, the films displayed the PL maximum peak at $\lambda_{max} \approx 530$ nm, which was exactly same as those of oleic acid-stabilized QD or PS–N_3–SH–QD dispersed in toluene (see Supporting Information, Figure S6). In addition, the films were observed to emit fluorescent light that is clearly detectable with the naked eye under irradiation of a low power hand-held UV lamp. These results also indicate that photo-crosslinking and excess UV treatment for the preparation of hydrophobic/hydrophilic multilayers do not cause the notable blue shift in the PL bands and the strong quenching effect due to relatively short UV exposure time. This approach is very simple and efficient when compared to conventional LbL methods based on electrostatic interaction which is complicated by a serious PL quenching and the solution stability (i.e., the small ligands with thiol and carboxylic acid groups or the control of solution pH).[31–33]

Figure 5b shows the change in the UV–Vis spectra occurred from (PAH/spiropyran-BCM)$_{10}$ multilayers before and after UV irradiation. This means that upon irradiation with 375 nm UV light for 6 min, the UV–Vis absorption spectra of (PAH/spiropyran-BCM)$_{10}$ films containing spiropyran showed a decrease in the absorption peak at 367 nm (spiropyran form) and the growth of a new absorption peak at 552 nm (merocyanine form). After the build-up of

(PAH/spiropyran-BCM)$_{10}$ multilayers onto (PS−N_3−SH−QD:PS−N_3)$_{30}$-coated NaCl substrates, transparent free-standing multilayers showing photochromic properties under UV light irradiation can be produced by dissolving the NaCl substrate in water, as shown in Figure 4b. The photochromic intensity of these films can be significantly increased by increasing the number of deposition cycles or photochromic dye concentration within hydrophobic PS core block of BCMs. Additionally, although the thickness of the free-standing film formed from a PS−N_3−SH−QD (1 wt.-% for QDs and 2 wt.-% for PS−N_3−SH): PS−N_3 (2 wt.-% for PS−N_3) blending solution was approximately 4 μm, these thicknesses could be decreased to approximately 1 μm by decreasing the solution concentration and layer number of PS−N_3−SH−QD:PS−N_3. Furthermore, the build-up of electrostatic multilayers in aqueous medium onto PS−N_3−SH−QD:PS−N_3 multilayer-coated NaCl substrates clearly shows that PS−N_3−SH−QD:PS−N_3 multilayers can effectively prevent the infiltration of water molecules into a NaCl substrate. As a result, our approach produces the free-standing optical films with both the highly PL properties by incorporating QDs into hydrophobic multilayers and the photochromic properties by inserting spiropyran dyes within electrostatically charged BCM multilayers.

Conclusion

A variety of free-standing functional films composed of hydrophobic and hydrophilic multilayers could be prepared easily on sacrificial ionic substrates without physical or chemical damage by photo-crosslinking and electrostatic LbL assembly. The desired properties (i.e., flexibility control and functionalities such as electrochemical or photoluminescent/photochromic properties) of the free-standing films could be controlled by the multilayer design and functionality of the components inserted. Similar to the LbL techniques developed thus far (i.e., LbL patterning using an electrostatic interaction in aqueous media), this approach based on photo-crosslinking and electrostatic interactions highlights the possibility of electrostatically patterned multilayers onto PS−N_3 multilayer-coated substrates. As a result, this approach is compatible with the typical LbL techniques, and can provide a more facile route to potential applications, such as free-standing electronic or optical films than the conventional LbL process.

Acknowledgements: This work was supported by KOSEF grant funded by the *Korea government* (2008-0058617), "SystemIC2010" project of the *Ministry of Knowledge Economy*, ERC Program of KOSEF grant funded by the *Korea government* (R11-2005-048-00000-0) and the Korea Research Foundation Grant funded by the *Korean government* (KRF-2008-D00264, KRF-2009-0074767, KRF-2009-0069813).

Received: February 23, 2010; Published online: 17 May 2010; DOI: 10.1002/macp.201000104

Keywords: catalase; crosslinking; free-standing film; hydrophobic multilayer; layer-by-layer; photo-crosslinking; polyelectrolyte; quantum dots

[1] H. H. Rmaile, J. B. Schlenoff, *J. Am. Chem. Soc.* **2003**, *125*, 6602.
[2] P. Podsiadlo, A. K. Kaushik, E. M. Arruda, A. M. Waas, B. S. Shim, J. D. Xu, H. Nandivada, B. G. Pumplin, J. Lahann, A. Ramamoorthy, N. A. Kotov, *Science* **2007**, *318*, 80.
[3] D.-H. Kim, J.-H. Ahn, W. M. Choi, H.-S. Kim, T.-H. Kim, J. Song, Y. Y. Huang, Z. Liu, C. Lu, J. A. Rogers, *Science* **2008**, *320*, 507.
[4] R. Vendamme, S. Y. Onoue, A. Nakao, T. Kunitake, *Nat. Mater.* **2006**, *5*, 494.
[5] C. Nardin, M. Winterhalter, W. Meier, *Langmuri* **2000**, *16*, 7708.
[6] Z. Tang, N. A. Kotov, S. Magonov, B. Ozturk, *Nat. Mater.* **2003**, *2*, 413.
[7] J. L. Lutkenhaus, K. D. Hrabak, K. McEnnis, P. T. Hammond, *J. Am. Chem. Soc.* **2005**, *127*, 17228.
[8] J. K. Ferri, W.-F. Dong, R. Miller, H. Mowhald, *Macromolecules* **2006**, *39*, 1532.
[9] N. I. Kovtyukhova, B. R. Martin, J. K. N. Mbindyo, P. A. Smith, B. Razavi, T. S. Mayer, T. E. Mallouk, *J. Phys. Chem. B* **2001**, *105*, 8762.
[10] G. Decher, *Science* **1997**, *277*, 1232.
[11] F. Caruso, R. A. Caruso, H. Möhwald, *Science* **1998**, *282*, 1111.
[12] T. C. Wang, R. E. Cohen, M. F. Rubner, *Adv. Mater.* **2002**, *14*, 1534.
[13] S. Y. Yang, M. F. Rubner, *J. Am. Chem. Soc.* **2002**, *124*, 2100.
[14] G. K. Such, J. F. Quinn, A. Quinn, E. Tjipto, F. Caruso, *J. Am. Chem. Soc.* **2006**, *128*, 9318.
[15] S. Lee, B. Lee, B. J. Kim, J. Park, W. K. Bae, K. Char, C. J. Hawker, J. Bang, J. Cho, *J. Am. Chem. Soc.* **2009**, *131*, 2579.
[16] J. Park, J. Kim, S. Lee, J. Bang, B. J. Kim, Y. S. Kim, J. Cho, *J. Mater. Chem.* **2009**, *19*, 4488.
[17] D. Buttry, *Advances in Electroanalytical Chemistry: Applications of the QCM to Electrochemistry*, Marcel Dekker, New York 1991.
[18] D. Zhang, S. M. Dougal, M. S. Yeganeh, *Langmuir* **2000**, *16*, 4528.
[19] B. Lee, Y. Kim, S. Lee, Y. S. Kim, D. Wang, J. Cho, *Angew. Chem. Int. Ed.* **2009**, DOI: 10.1002/anie.200905596.
[20] J. Park, I. Kim, H. Shin, M. J. Lee, Y. S. Kim, J. Bang, F. Caruso, J. Cho, *Adv. Mater.* **2008**, *20*, 1843.
[21] T. You, O. Niwa, M. Tomita, S. Hirono, *Anal. Chem.* **2003**, *75*, 2080.
[22] B. K. Jena, C. R. Raj, *Anal. Chem.* **2006**, *78*, 6332.
[23] S. Hrapovic, Y. Liu, K. B. Male, J. H. T. Luong, *Anal. Chem.* **2004**, *76*, 1083.
[24] W. Jin, X.-Y. Shi, F. Caruso, *J. Am. Chem. Soc.* **2001**, *123*, 8121.
[25] A. Yu, F. Caruso, *Anal. Chem.* **2003**, *75*, 3031.
[26] S. S. Shiratori, M. F. Rubner, *Macromolecules* **2000**, *33*, 4213.

DOI: 10.1002/macp.201000104

[27] J. Park, I. Kim, H. Shin, M. J. Lee, Y. S. Kim, J. Bang, F. Caruso, J. Cho, *Adv. Mater.* **2008**, *20*, 1843.
[28] J.-S. Lee, J. Cho, C. Lee, I. Kim, J. Park, Y. Kim, H. Shin, J. Lee, F. Caruso, *Nat. Nanotechnol.* **2007**, *2*, 790.
[29] J. Cho, H. Hong, K. Char, F. Caruso, *J. Am. Chem. Soc.* **2006**, *128*, 9935.
[30] R. A. Evans, *Nat. Mater.* **2005**, *4*, 249.
[31] I. L. Medintz, H. T. Uyeda, E. R. Goldman, H. Mattoussi, *Nat. Mater.* **2005**, *4*, 435.
[32] V. R. Hering, G. Gibson, R. I. Schumacher, A. Faljoni-Alario, M. J. Politi, *Bioconjugate Chem.* **2007**, *18*, 1705.
[33] H. Mattoussi, J. M. Mauro, E. R. Goldman, G. P. Anderson, V. C. Sundar, F. V. Mikulec, M. G. Bawendi, *J. Am. Chem. Soc.* **2000**, *122*, 12142.